IEEE Access
Multidisciplinary ⋮ Rapid Review ⋮ Open Access Journal

Received 30 May 2023, accepted 27 June 2023, date of publication 3 July 2023, date of current version 11 July 2023.

Digital Object Identifier 10.1109/ACCESS.2023.3291590

RESEARCH ARTICLE

Optimal Placement and Capacity of Battery Energy Storage System in Distribution Networks Integrated With PV and EVs Using Metaheuristic Algorithms

NATSAWAT POMPERN[1], (Member, IEEE), SUTTICHAI PREMRUDEEPREECHACHARN[1], APIRAT SIRITARATIWAT[2], AND SIROTE KHUNKITTI[1]

[1]Department of Electrical Engineering, Faculty of Engineering, Chiang Mai University, Chiang Mai 50200, Thailand
[2]Department of Electrical Engineering, Faculty of Engineering, Khon Kaen University, Khon Kaen 40002, Thailand

Corresponding author: Sirote Khunkitti (sirote.khunkitti@cmu.ac.th)

This work was supported and funded by Provincial Electricity Authority-Graduate School, Chiang Mai University program.

ABSTRACT In this research, the optimal placement and capacity of battery energy storage systems (BESS) in distribution networks integrated with photovoltaics (PV) and electric vehicles (EVs) have been proposed. The main objective function is to minimize the system costs including installation, replacement, and operation and maintenance costs of the BESS. The replacement cost has been considered over 20 years while the operation and maintenance costs are the costs incurred by transmission line loss, voltage regulation, and peak demand. To solve the problem, three metaheuristic algorithms, namely particle swarm optimization (PSO), african vultures optimization algorithm (AVOA), and salp swarm algorithm (SSA), are employed. The proposed approach is evaluated on the IEEE 33- and 69-bus distribution systems integrated with PV and EVs. The results provided by the considered algorithms are compared in terms of the objective function, system efficiency enhancement, payback period, and statistical analysis. The simulation results show that after the BESS installation, the voltage profile can be improved, transmission loss is reduced, and peak demand is decreased where PSO provides the best objective values and AVOA achieves the fastest payback periods in both systems.

INDEX TERMS Battery energy storage systems, photovoltaics, electric vehicles, metaheuristic algorithms, particle swarm optimization, African vultures optimization algorithm, salp swarm algorithm.

I. INTRODUCTION

At present, energy consumption tends to continuously increase because of economic growth and advanced industrial development technology making electric power an important factor in driving the economy and the quality of life of people in many countries [1], [2], [3]. Moreover, electric vehicle (EV) and solar power generation industries, which significantly impact the economy and electricity generation, have been continuously growing [4], [5], [6]. The increasing number of EVs needs a greater number of EV charging stations affecting distribution systems to be vulnerable. Photovoltaic (PV) is becoming commonplace in our daily lives and has been integrated into electric power distribution systems supporting distribution systems to supply loads and improve voltage profile and harmonic distortion (THD), etc. [7], [8]. So that, to support the increase of electricity consumption from EVs and load growth, the efficiency of the distribution systems integrated with PV is aimed to be enhanced by using an energy storage system (ESS) for storing energy from PV and grid when demand is low and supply it back to the grid during high demand period.

The technology of ESS for installation in distribution systems is chosen depending on several factors such as energy

The associate editor coordinating the review of this manuscript and approving it for publication was Jiefeng Hu.

capacity, efficiency, cost, advantages, disadvantages, and credibility of the ESS [9]. In addition, the ESS selected to be installed in the distribution systems should take a moderate amount of time to discharge (minutes-hours), because this discharging time can respond to daily loads in a timely manner [10].

By installing BESSs in distribution systems, the efficiency of the distribution systems can be improved depending on the placement and capacity of the BESS. Finding the best appropriate placement and capacity of the BESS is thus an important task that must be studied and considered to improve distribution system performance and reliability of power generation and also minimize system costs. Several works have studied many methods to determine the best appropriate placement and capacity of the BESS. In [11], Boonluk et al. presented the optimal placement and capacity of the BESS together with renewable energy sources (RESs) by using genetic algorithm (GA) and particle swarm optimization (PSO) to determine the lowest system costs in the IEEE 33-bus distribution network, and it was found that PSO is more effective than GA. In [12], Fathy. proposed a novel artificial hummingbird algorithm (AHA) to determine the optimal locations and sizes of biomass-based distributed generators (DGs) in radial distribution networks in order to minimize active power loss and voltage deviation. It was found that the proposed algorithm could significantly enhance network performance in terms of power loss and voltage deviation reductions. In [13] Tolba et al. introduced an effective optimization method called modified forensic-based investigation (mFBI) optimizer to determine the optimal location and capacity of DGs in the IEEE 118-bus system and real distribution system in Delta-Egypt. The optimization process was based on a multi-objective function aiming to minimize power losses, overall node voltage deviation and total annual operational costs, and maximize voltage stability margin. The results demonstrate that the mFBI optimizer outperforms other existing techniques, providing superior outcomes in terms of the specified objectives. Jayasekara et al. introduced the optimal installation of the BESS together with PVs and winds turbines (WTs) by using the interior point method for controlling operation together with data management system (DMS) and energy management system (EMS) in the IEEE 33-bus distribution system to minimize distribution system costs and battery cycling cost [14]. The results showed that the BESS can improve the efficiency of the distribution system evaluated by examining voltage regulation enhancement, decreasing loss, and decreasing peak demand. Mazza et al. considered finding the optimal placement and capacity of the BESS connected with EVs and DGs by using GA and greedy algorithm to minimize investment and operation and maintenance (O&M) costs in a rural 22-bus distribution system which is a low voltage grid [15]. In [16], Ahmadian presented the optimal BESS installation by using a fuzzy model to predict the uncertainty of load profile, and tabu search (TS) and simulated annealing (SA) algorithms were applied to find the power of DGs, the number of battery units, power rating of BESS, and capacity and locating of the BESS in the multi-objective problems where the objectives included costs of electrical energy purchased by distribution utility and power loss in the distribution network. In [17], Khalid et al. introduced the optimal placement and capacity of DGs and BESS in a stand-alone microgrid 17-bus system connected with residential and EV loads by using teaching learning-based optimization (TLBO). The results showed that losses in the system could be decreased, and voltage quality is improved. Zheng et al. indicated the optimal number, placement, and sizes of the BESSs in radial distribution systems to control voltage regulation and minimize life cycle costs by using a hierarchical planning model and natural aggregation algorithm (NAA) [18]. Thus, several methods have been used to determine the optimal placement and capacity of the BESS in the distribution systems in order to reduce system costs such as installation, replacement, transmission loss, voltage regulation, and peak demand costs. However, most of them have only considered some of the system costs although all the system costs are important, and traditional algorithms have been used to solve the problems in most studies.

So, several works presented the optimal placement and capacity of the BESS for distribution systems by considering all of the system costs, and some new efficient optimization algorithms were employed. In [19], Khunkitti et al. proposed the optimal placement and sizing of the BESS for distribution networks connected with DGs by using GA, PSO, and SSA algorithms to minimize system costs including transmission loss, voltage regulation, and peak demand costs in the IEEE 33- and 69-bus distribution systems. The results presented the BESS could mitigate the system costs, improve the voltage profile, decrease power losses, and decrease peak demand. However, this research only considered the price of operation and maintenance of distribution systems, which did not include the costs of battery installation and replacement. In addition, Janamala et al. proposed an approach to optimally integrate interline-PV (I-PV) systems under different EV load penetration levels by aiming at real power loss reduction and voltage profile enhancement [20]. The coyote optimization algorithm (COA), PSO, and grey wolf optimizer (GWO) were used to determine the optimal solutions. The simulation results presented that I-PV could be used to improve the voltage profile, decrease transmission loss, and adapt to real-world situations; however, this paper only considered I-PV installations where PV and BESS were installed at the same placement, and the BESS installation costs were not included. In [21], Sadeghi presented the optimal installation of BESS together with DGs and EVs by using multi-objective PSO (MOPSO) and Monte Carlo simulation (MCS) to find optimal life cycle costs (LCCs) consisting of initial cost (IC), maintenance cost (MC), and replacement cost (RC), and the results showed that the LCC could be decreased.

Although various works have studied the optimal placement and capacity of the BESS installation, most of them

have not considered battery installation and replacement costs as in [19] and [20], and some of them used traditional optimization algorithms [21]. Thus, this work presents the optimal placement and capacity of the BESS in distribution networks connected with PV and EVs by considering system costs as the objective function. A traditional efficient optimization algorithm which is PSO [22] and new efficient algorithms which are AVOA [23] and SSA [24] are employed to determine the optimal solutions.

This work's primary contributions can be summarized as:

1) The study aims to determine the optimal placement and capacity of the BESS in the IEEE 33- and 69-bus distribution systems connected with PV and EV penetrations by considering overall system costs, which include investment, replacement, operation, and maintenance costs as the objective function to be minimized.

2) The efficiency of the distribution systems is enhanced by decreasing transmission line loss, decreasing peak demand, and improving voltage profile after the BESS installation.

3) Three mentioned optimization algorithms are utilized to find solutions to the problems, and their efficiency is evaluated through a comparative analysis.

4) The break-even point for investing in the BESS installation is calculated for investment decisions, and the statistical analysis is considered to validate the performance of each algorithm. The content has been arranged in topical order as follows: Section II presents the ESS installation in a distribution system. In Section III, the problem is defined and described. The outlines of the metaheuristic algorithms and their implementation are explained in Section IV. Section V depicts the results and discussions. The work is finally concluded in Section VI.

II. ENERGY STORAGE SYSTEMS IN A DISTRIBUTION SYSTEM

ESS are terms used to describe systems or equipment installed in a system in order to convert electrical energy into other energy types such as electrochemical, mechanical, chemical, thermochemical, and thermal energies that can be stored and converted back into electrical energy again when needed [10], [25], [26], [27]. In this research, BESS which, applies the energy conversion between electrical energy and electrochemical energy, is used to be installed in the distribution systems because of its suitable discharging time that can respond to daily loads in a timely manner. The BESS and its simulation are described in the following subsection.

A. BATTERY ENERGY STORAGE SYSTEMS (BESSs)

The BESSs take a moderate amount of time to discharge (about minutes to hours) with a ratio between 1 and 10, meaning that there is a capacity of 1–10 kWh for a system with a power of 1 kW. Examples of the BESSs are lead acid batteries (LA), lithium-ion batteries (Li-ion), redox flow batteries (RFB), and sodium sulphur batteries (NaS). The Li-ion battery has been chosen in this study because of its several advantages such as high efficiency of more than 90 %, high energy density (90-190 Wh/kg), up to 10,000 cycle times, and suitable cost.

There are several factors affecting the service life of the Li-ion batteries in the BESS, which should be considered, including temperature, the operation cycle numbers of the BESS, and depth of discharge (DOD) [11]. The BESS life can be increased by carefully controlling heat dissipation at the optimal temperature which is around 15–35 degrees Celsius, avoiding charging and discharging frequently. Frequent charging and discharging should be avoided. The DOD of the Li-ion is recommended at 80% of the total capacity. The rates of charge and discharge should not be too high because it will cause high temperatures to the BESS, which will result in a shorter service life [28], [29].

B. BATTERY ENERGY STORAGE SYSTEM SIMULATION

The simulation of the BESS considers the charging and discharging of the BESS at equal intervals within 24 hours [11], [14], [19]. The period is divided equally into 1 hour 30 minutes or 15 minutes, so BESS can support the battery charging and discharging rate at a value of 24, 48, or 96 respectively. The charging and discharging rates in any period are C_{iT}, which can be determined according to the following equation:

$$C_{iT} = \begin{bmatrix} E_B(1) \\ \vdots \\ E_B(m) \end{bmatrix} \tag{1}$$

where $E_B(t)$ represents the energy in the BESS (MWh) at time $t = 1, 2, 3, \ldots,$ m.

The Fourier series is used to find the energy in the BESS by using the Fourier coefficient vector (C_{iF}) provided by the optimization process. The Fourier series is adopted in this work because it can be utilized to find the energy in the BESS expressed in finely dispersed periodic patterns. By using the Fourier series, the periodic pattern can be divided into a group of sinusoidal components in the time domain enabling a thorough analysis of the energy of the BESS [30]. The method is to start at random with 16 Fourier coefficient values and use the Fourier transform to predict the BESS's electrical energy (EB) every hour. The Fourier series is then used to represent the state of energy (SOE) over the entire considered period. The energy in the BESS is determined by using the presented equations [14], [30].

$$C_{iF} = \begin{bmatrix} a_1, b_1 \\ \vdots \\ a_n, b_n \end{bmatrix} \tag{2}$$

$$E_B(t) = a_0 + a_1 \cos\left(\frac{2\pi t}{T}\right) + b_1 \sin\left(\frac{2\pi t}{T}\right) + \cdots + a_n \cos\left(\frac{2\pi nt}{T}\right) + b_n \sin\left(\frac{2\pi nt}{T}\right) \tag{3}$$

where C_{iF}, a_0, a_n, b_n, n, t, and T are the Fourier coefficient vector, constant Fourier coefficient, Fourier cosine coefficient, Fourier sine coefficient, number of Fourier coefficients

which is set to 8, time, and period, respectively. The Fourier cosine and sine coefficients are the optimization variables for the problem.

The energy in the BESS, $E_B(t)$ is obtained by substituting C_{iF} from (2) into (3). From (3), a_0 is not required because the constant a_0 has no impact on the charging and discharging of the BESS and has no impact on the daily energy cost coefficient. So, it can be set after an optimization process to ensure that the BESS power curve is not below the minimum value required to perform the DOD requirements.

The energies' variation in the BESS at two consecutive times is computed by (4) in order to find the power of the BESS as in (5) and (6). The power of the BESS can then be used to indicate the state of the BESS. When the BESS is in a charging state, the BESS power is positive, indicating the energy being added to the BESS. Conversely, when the BESS is in a discharging state, the BESS power is negative, indicating the energy being released from the BESS.

$$\Delta E_B = E_B(t) - E_B(t-1) \tag{4}$$

$$P_B(t) = \Delta E_B / (\Delta t \times \eta_c), P_B(t) > 0 \tag{5}$$

$$P_B(t) = (\Delta E_B \times \eta_d) / \Delta t, P_B(t) < 0 \tag{6}$$

where ΔE_B is the energies' variation in the BESS at two consecutive times, $\eta_c = \eta_d = \sqrt{\eta_{bat}}, \eta_{bat} = 0.9$ is the BESS efficiency in a cycle, and η_c, η_d, P_B, and Δt are the BESS charging efficiency, BESS discharging efficiency, BESS power, and sampling interval time, respectively.

C. OPTIMAL CAPACITY OF THE BESS

To find the optimal capacity of the BESS, the power capacity and energy capacity should be considered to decrease the total costs and maintain the quality and reliability of distribution systems. Moreover, the number of cycles and the SOC should also be considered because they are two main factors that affect the BESS life [9]. By improving the BESS's charging and discharging cycles, the daily SOC swings can be decreased, which helps increase the efficiency of the BESS's life cycle. The size of the BESS can be calculated by the difference between the maximum and minimum energy in the BESS divided by the maximum DOD as shown below.

$$Battery\,size(kWh) = \frac{\left|E_B^{\max} - E_B^{\min}\right|}{DOD_{\max}} \tag{7}$$

where $DOD_{\max} = 0.8$, $E_B^{\max}$ and $E_B^{\min}$ are the maximum and minimum values of energy in the BESS, respectively.

The BESS daily cycle and service life cycle can be estimated from (8) and (9), respectively.

$$Cycles = \frac{1}{2}\left(\frac{\sum_{t=1}^{T} E_B(t) - E_B(t-1)}{DOD_{\max} \times Battery\,size}\right) \tag{8}$$

$$Q(years) = \frac{CyclesLife}{Cycles \times D} \tag{9}$$

where Cycles, D = 285 days [14], Cycle Life = 3,000 cycles [14], and Q are the number of daily BESS cycles, number of BESS operating days, number of cycles in the nominal cycle life of Li-ion battery, and actual service life cycle in years, respectively.

III. PROBLEM FORMULATION

To determine the optimal placement and capacity of the BESS in distribution networks connected with PV and EV charging stations, the costs of installation, replacement, transmission loss, voltage regulation, and peak demand in the distribution systems are considered as the objective function to be minimized while the constraints are the voltages of all buses and BESS power and energy.

A. OBJECTIVE FUNCTION

The objective function of this research is to decrease the total costs of BESS installation (C_{system}) including investment cost (C_{IC}), replacement cost (C_{RC}), and operation and maintenance costs (C_{MC}) [17], [18], [19]. The size of the BESS will affect the investment cost while the replacement cost varies depending on the size and life cycle time of the BESS. Moreover, the operation and maintenance costs of the distribution systems include voltage regulation cost (C_{CVR}), transmission loss cost (C_{loss}), and peak demand cost (C_p). Equation (10) represents the objective function of this work, which can be obtained from (11) – (17).

$$f(C_{iF}) = \min\left(C_{system}\right) \tag{10}$$

$$C_{system} = C_{IC} + C_{MC} + C_{RC} \tag{11}$$

$$C_{IC} = N_{bat} \times \gamma_{IC} \tag{12}$$

$$C_{MC} = C_{CVR} + C_{loss} + C_p \tag{13}$$

$$C_{CVR} = \left(\sum_{t=1}^{T}\sum_{i=1}^{N} \left|V_i - V_{ref}\right|\right) \times \gamma_{VR} \tag{14}$$

$$C_{loss} = \left(\sum_{t=1}^{T}\sum_{i=1}^{M} \left|Lineloss\right|\right) \times \gamma_{loss} \tag{15}$$

$$C_p = P_{\max} \times \Delta t \times \gamma_p \tag{16}$$

$$C_{RC} = N_{bat} \times \gamma_{IC} \times \frac{t_{year}}{Cycles} \tag{17}$$

where N_{bat}, N, T, V_i, V_{ref}, M, $Lineloss$, $P_{\max}$, γ_{VR}, γ_{loss}, γ_p, γ_{IC}, and t_{year} are the BESS size (kWh), total number of buses, period, voltage at bus i (p.u.), reference voltage which is 1 p.u., total number of branches, actual power loss in each line, maximum power demand, rate of voltage regulator cost ($\gamma_{VR} = 0.142$ \$/p.u. [14], [19]), rate of transmission loss cost ($\gamma_{loss} = 0.284$ \$/kWh [14], [19]), rate of maximum energy demand cost ($\gamma_p = 200$ \$/kWh/year [14], [19]), rate of BESS installation cost ($\gamma_{IC} = 100$ \$/kWh [31]), and duration of this study ($t_{year} = 20$ years), respectively.

B. CONSTRAINTS

1) INEQUALITY CONSTRAINTS

Voltage conditions of each bus must be within the range of ±10% of the reference voltage as follows:

$$V_{\min} \le V_i^t \le V_{\max} \tag{18}$$

where $V_{\min}$ and $V_{\max}$ are the minimum and maximum voltages of each bus, respectively, and V_i^t is the voltage at bus i at each time t.

In addition, the power and capacity of the BESS are limited to prevent the BESS from being harmed during charging and discharging, which can be expressed by the following equations.

$$PB_{\min} \leq P_{cha}^t, P_{dis}^t \leq PB_{\max} \tag{19}$$

$$EB_{\min} \leq EB^t \leq EB_{\max} \tag{20}$$

where PB_{min} and PB_{max} represent the minimum and maximum powers of the BESS, respectively. Recent charging and discharging powers of the BESS at time t are represented by P_{cha}^t and P_{dis}^t, respectively, and the minimum and maximum capacities of the BESS are $EB_{\min}$ and $EB_{\max}$, respectively.

2) EQUALITY CONSTRAINT

For the equality constraint, the power balance is controlled in each bus of a distribution system as shown in the equation below [20].

$$P_{grid}(t) = P_D(t) - P_{pv}(t) \pm P_B(t) - P_L(t) \tag{21}$$

where $P_{grid}, P_D, P_{pv}, P_B$, and P_L are grid power, load demand power, PV power, BESS power, and transmission line power loss, respectively.

IV. METAHEURISTIC ALGORITHMS AND IMPLEMENTATION

In this research, to determine the optimal placement and capacity of the BESS in distribution systems connected with PV and EVs, three metaheuristic algorithms including PSO, AVOA, and SSA are adopted. The effectiveness of these algorithms is compared in terms of voltage deviation index (VDI), power losses, and peak demand enhancement. The implementation of the whole process is explained in the following subsections.

A. PARTICLE SWARM OPTIMIZATION (PSO)

PSO is one of the most widely used techniques for solving optimization problems because of its simplicity and high efficiency in searching for solutions. Although PSO is a traditional method, it could overcome newly proposed optimization algorithms in some works [19], [32], [33]. So, it is possible that PSO can be better than modern algorithms in this work. PSO was proposed by Kennedy and Eberhart inspired by the social behavior of a group of fishes or birds looking for food [22]. In the PSO simulation, firstly, the position and speed of each particle are randomly initialized. Each particle i then keeps the best answer in each iteration called personal best (p_{best}). All particles share their best answer obtained so far, such that a single particle has access to the most effective solution among all particles called global best (g_{best}) in order to adjust its position and speed to the best solution. The velocity and position of the i^{th} particle are updated by the following equations.

$$v_i^{k+1} = w_i^k \times v_i^k + c_1 r_1 (p_{best,i}^k - x_i^k) + c_2 r_2 (g_{best}^k - x_i^k) \tag{22}$$

$$x_i^{k+1} = x_i^k + v_i^{k+1} \tag{23}$$

where the velocities of the i^{th} particle at iterations $k+1$ and k are denoted by v_i^{k+1} and v_i^k, respectively. x_i^{k+1} and x_i^k represent the positions of the i^{th} particle at iterations $k+1$ and k, respectively, c_1 and c_2 are both positive acceleration coefficients set to 2. r_1 and r_2 are two uniformly randomly produced numbers between [0,1]. $p_{best,i}^k$ is the personal best position of the i^{th} particle at iteration k, g_{best}^k refers to the global best position of all particles during the k^{th} iteration, and w is the inertia weight at the k^{th} iteration calculated by the equation below.

$$w = w_{\max} - \left(\frac{w_{\max} - w_{\min}}{iter_{\max}} \times iter\right) \tag{24}$$

where $w_{\max}$ is set to 0.9, $w_{\min}$ is set to 0.4, $iter$ is the current iteration number, and $iter_{\max}$ is the maximum iteration number.

B. AFICANS VULTURES OPTIMIZATION ALGORITHM (AVOA)

AVOA is a meta-heuristic algorithm inspired by African vultures that migrate in flocks to locate food and cohabit where the food location indicates the best solution. The AVOA begins with a random sampling of the vultures' initial positions in the problem area, and the best two vultures are evaluated by the following equation.

$$R(i) = \begin{cases} BestVulture_1 if\ p_i = L_1 \\ BestVulture_2 if\ p_i = L_2 \end{cases} \tag{25}$$

$$p_i = \frac{F_i}{\sum_{i=1}^{n} F_i} \tag{26}$$

where $R(i)$ is one of the best vultures selected, p_i is the probability of choosing the best solution, n is the number of group's vulture, L_1 and L_2 are the indicators calculated before the searching process, with the values in the range of 0 and 1, and the sum of them is equal to 1. The rates of starvation of both vultures are then calculated by the following equations.

$$F = (2 \times rand_1 + 1) \times z \times \left(1 - \frac{iter}{iter_{\max}}\right) + t \tag{27}$$

$$t = h \times \left(\sin^w\left(\frac{\pi}{2} \times \frac{iter}{iter_{\max}}\right) + \cos\left(\frac{\pi}{2} \times \frac{iter}{iter_{\max}}\right) - 1\right) \tag{28}$$

where F indicates the rate of starvation, $rand_1$ has a random value that varies between 0 and 1, $iter$ is the current iteration, $iter_{\max}$ is the maximum number of iterations, z is a randomly generated number in the range of [-1,1] regenerating in each iteration, t is adopted to improve the search process by avoiding the local optima, h is a number randomly chosen between -2 and 2, w is a parameter used to balance the exploration and

exploitation phases [23]. When z falls below zero in the range of [-1,0), the vulture is starved, and when it rises in the range of [0,1], the vultures are satiated.

If the vultures have a value of $F \geq 1$, then the vultures are satiated. Vultures will explore in search of food at random distances from one of the two groups and update the position by using the presented equations.

$$D(i) = |X \times R(i) - P(i)| \tag{29}$$

$$P(i+1) = R(i) - D(i) \times F \tag{30}$$

$$P(i+1) = R(i) - F + rand_2 \times ((ub - lb) \times rand_3 lb) \tag{31}$$

where $D(i)$ is a parameter used to update the position of the best vultures in two groups, X is the vultures move randomly to prevent food from others, $P(i)$ is the vulture position vector in iteration i, $P(i+1)$ is the vulture position vector in iteration $i+1$, $rand_2$ and $rand_3$ are random number generated between [0,1], and lb and ub illustrate the lower and upper limits of the variables.

Vultures are quite full and very active if $0.5 \leq F < 1$. As a result, there will be violent disputes between vultures, with aggressive vultures refusing to share their meal. Weak vultures receive food scraps from stronger vultures by updating the position of the vulture by using the given equations.

$$d(t) = R(i) - P(i) \tag{32}$$

$$P(i+1) = D(i) \times (F + rand_4) - d(t) \tag{33}$$

$$S_1 = R(i) \times \left(\frac{rand_5 \times P(i)}{2\pi}\right) \times \cos(P(i)) \tag{34}$$

$$S_2 = R(i) \times \left(\frac{rand_6 \times P(i)}{2\pi}\right) \times \sin(P(i)) \tag{35}$$

$$P(i+1) = R(i) - (S_1 + S_2) \tag{36}$$

where $d(t)$ is the distance between the vulture and one of the best vultures from the two groups, S_1 and S_2 are a spiral equation generated between all vultures and one of the two best vultures, and $rand_4$, $rand_5$, and $rand_6$ are random numbers in the range of [0,1].

When the vulture's hunger level is $F < 0.5$, it assumes a situation in which the number of vultures is more than the number of foods resulting in conflicts between vultures. The food is usually in one place, and all the vultures tend to fly there. Different equations are applied to update the vulture position, and the best foraging response is then produced as shown in the equations below.

$$A_1 = BestVulture_1(i) - \frac{BestVulture_1(i) \times P(i)}{BestVulture_1(i) - P(i)^2} \times F \tag{37}$$

$$A_2 = BestVulture_2(i) - \frac{BestVulture_2(i) \times P(i)}{BestVulture_2(i) - P(i)^2} \times F \tag{38}$$

$$P(i+1) = \frac{A_1 + A_2}{2} \tag{39}$$

$$P(i+1) = R(i) - |d(t)| \times F \times Levy(d) \tag{40}$$

where A_1 and A_2 are great deals of competition for food that may accumulate various species of vultures on one food source, $BestVulture_1(i)$ is the best vulture of the first group in iteration i, $BestVulture_2(i)$ is the best vulture of the second group in iteration i, Levy(d) is a Levy flight used to increase the randomness of the AVOA computed by the given equation.

$$Levy(d) = 001 \times \frac{u \times \sigma}{|v|^{\frac{1}{\beta}}}, \sigma = \left(\frac{\Gamma(1+\beta) \times \sin(\frac{\pi\beta}{2})}{\Gamma(1+2\beta) \times \beta \times 2(\frac{\beta-1}{2})}\right)^{\frac{1}{\beta}} \tag{41}$$

where u and v are random numbers in the range of [0,1], and β is equal to 1.5.

C. SALP SWARM ALGORITHM (SSA)

SSA is a metaheuristic algorithm inspired by the chain motion of the salps in the deep ocean. By classifying salps into two groups, leaders and followers, the leaders are at the front of the chain and the rest of the salps are followers. The leader guides them to approach the food source, represented by the variable F in the n-dimensional search area, which is the number of variables in each problem. To update the position of the leader, the following equation is applied.

$$x_j^1 = \begin{cases} F_j + c_1((ub_j - lb_j)c_2 + lb_j), & c_3 \geq 0 \\ F_j - c_1((ub_j - lb_j)c_2 + lb_j), & c_3 < 0 \end{cases} \tag{42}$$

where x_j^1 represents the leader's position of the swarm in the j^{th} dimension, F_j represents the food source in the j^{th} dimension, ub_j is the upper bound of the j^{th} dimension, lb_j is the lower bound of the j^{th} dimension, and c_2, and c_3 are randomly generated numbers.

The parameter c_1 is an important parameter in SSA used to balance the exploration and exploitation phases which can be calculated by the given equation.

$$c_1 = 2e^{-(\frac{4iter}{iter_{\max}})^2} \tag{43}$$

where $iter$ is the current iteration and $iter_{max}$ is the maximum iteration number.

The parameters c_2 and c_3 are random numbers uniformly randomly generated in the range of [0,1] that determine the next position of the salp swarm.

To update the location of the follower group, Newton's laws of motion are applied where the time in optimization is the iteration, and the discrepancy between iterations is equal to 1 as expressed in the following equation.

$$x_j^i = \frac{1}{2}(x_j^i + x_j^{i-1}), i \geq 2 \tag{44}$$

where $i \geq 2$, x_j^i is the position of the i^{th} follower in the j^{th} dimension, x_j^{i-1} is the position of the followers in the j^{th} dimension.

D. DISTRIBUTION SYSTEM EFFICIENCY EVALUATION

In this research, distribution system efficiency is investigated after the BESS installation. The efficiency is investigated in terms of transmission loss, VDI, and peak demand, which are described in the following subsections.

1) VOLTAGE DEVIATION INDEX (VDI)

VDI is used to indicate the efficiency of the distribution system evaluated by examining voltage profile enhancement when installing the BESS. The VDI can be calculated by the percentage of the difference between the reference voltage and the actual voltage for the period as presented in the following equation.

$$\%VDI_i = \max_T \frac{|V_{ref} - V_i|}{V_{ref}} \times 100,$$
$$\%VDI = \sum_{i=1}^{N_{bus}} \%VDI_i \tag{45}$$

where $\%VDI_i$ is the maximum percentage of VDI at bus i for the period time T, V_{ref} is the reference bus voltage, V_{i} is the voltage at bus i, $\%VDI$ is the total percentage of VDI of the distribution system, and N_{bus} is the total number of buses.

2) TRANSMISSION LOSSES

The transmission losses consist of active power, reactive power, and apparent power losses, which are used to compare the efficiency of the system after the BESS installation calculated by the following equations.

$$P_{loss} = \sum_{t=1}^{T} \sum_{l}^{N_l} P_l^t,$$
$$Q_{loss} = \sum_{t=1}^{T} \sum_{l}^{N_l} Q_l^t,$$
$$S_{loss} = \sqrt{P_{loss}^2 + Q_{loss}^2} \tag{46}$$

where P_{loss}, Q_{loss}, and S_{loss} are the active power, reactive power, and apparent power losses for the period time T, respectively, P_l^{t}, Q_l^{t} are the active and reactive power losses of line l for the period time T.

3) PEAK DEMAND

Peak demand represents the maximum active power demand during the considered time interval which is 24 hours in this study. To further evaluate the efficiency enhancement of the distribution systems, the peak demand enhancement indicated by the peak shaving is investigated after the BESS installation.

E. IMPLEMENTATION

To determine the optimal solution, three metaheuristic algorithms consisting of PSO, SSA, and AVOA are employed to find the optimal placement and capacity of the BESS in distribution systems connected with PV and EV charging stations.

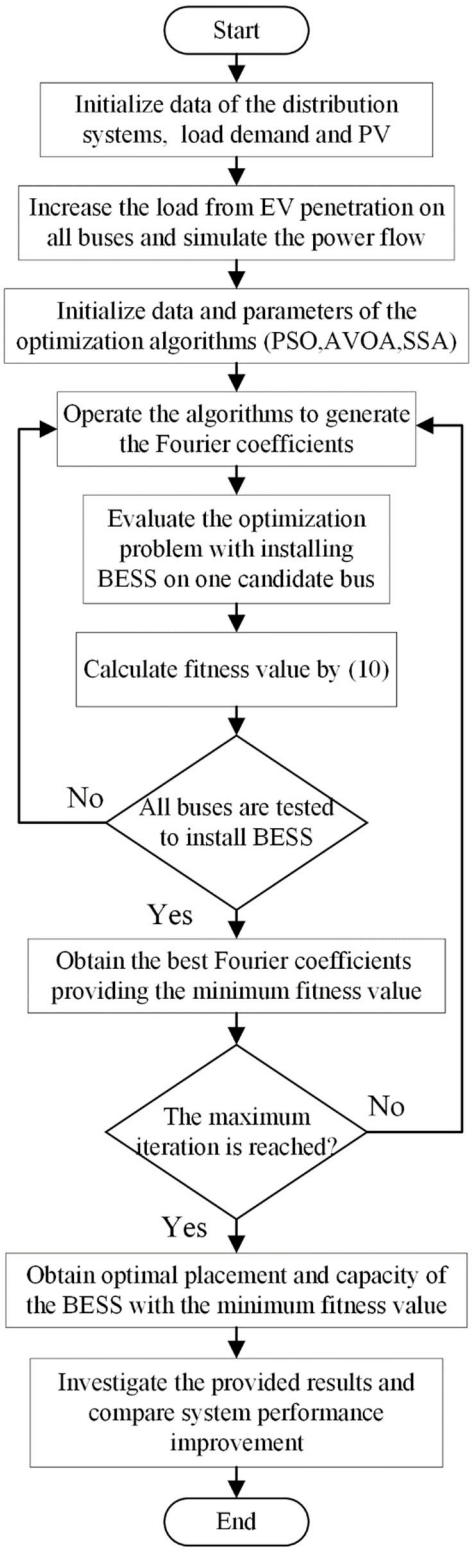

FIGURE 1. Implementation of the proposed method.

The implementation of the proposed method is depicted as a flowchart in Fig. 1, and the tested systems and EV modeling are described in the following subsections.

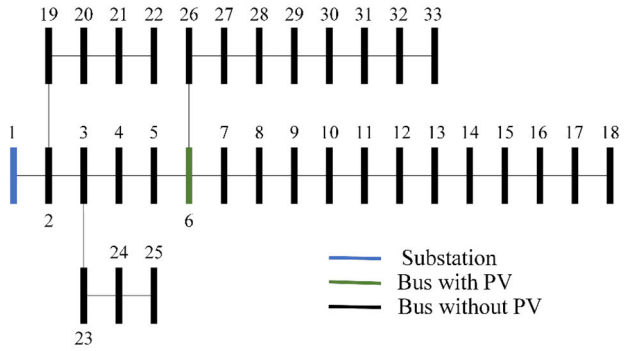

FIGURE 2. Single-line diagram of the IEEE 33-bus distribution system [34].

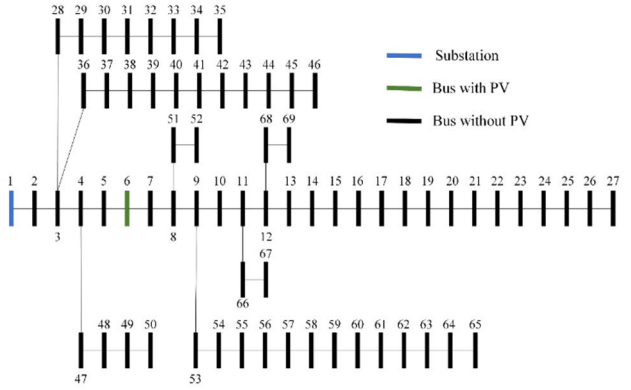

FIGURE 3. Single-line diagram of the IEEE 69-bus distribution system [35].

TABLE 1. Hourly load profile and PV generation profile in a typical day [20].

Hr	Load (p.u.)	PVp (p.u.)	Hr	Load (p.u.)	PVp (p.u.)
1	0.867	0	13	0.911	1.000
2	0.852	0	14	0.904	0.943
3	0.837	0	15	0.907	0.820
4	0.830	0	16	0.911	0.634
5	0.830	0	17	0.915	0.387
6	0.859	0	18	0.919	0.144
7	0.889	0	19	1.000	0
8	0.926	0.216	20	1.000	0
9	0.933	0.531	21	0.963	0
10	0.937	0.757	22	0.911	0
11	0.941	0.904	23	0.889	0
12	0.933	0.979	24	0.867	0

1) SYSTEM MODELING

The IEEE 33-bus and IEEE 69-bus distribution systems are adopted to determine the optimal placement and capacity of the BESS. The single-line diagrams of these systems are shown in Fig. 2 and Fig. 3, respectively [34], [35]. The base power is 10 MVA and the base voltage is 12.66 kV for both systems. The PV which is 5000 kW in this work was installed on the 6th bus which is the best bus for the PV installation as presented in [20]. The maximum load demand for the IEEE 33-bus and 69-bus systems are 3,715 kW and 3,802 kW

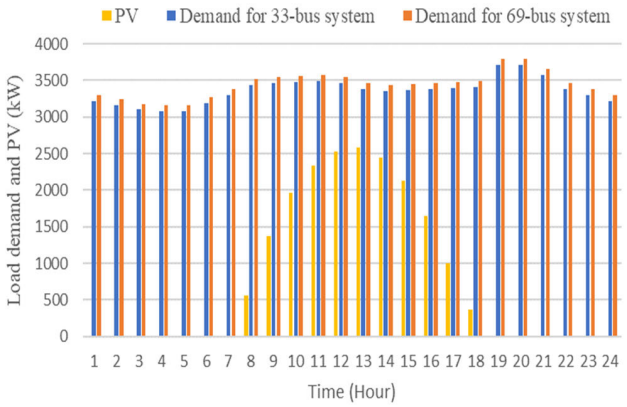

FIGURE 4. Load Demand and PV load profile of the considered distribution systems [20].

respectively. The load demands are presented as the 24 hours in p.u. of the base power at 2,070.86 kW as in Table 1. Fig. 4 presents the relationship between time and the amount of the original load demand, and the solar power generation capacity within a day of the IEEE 33-bus and IEEE 69-bus distribution systems.

2) MODELLING OF CHARGING STATIONS FOR EVs

To model the charging stations for EVs, EV load demand on all buses is assumed to be increased by using an AC/DC converter or charging port since the BESS and grid are used to supply power to the EVs by the penetration load [20], [36]. Equations (47) and (48) specify additional real and reactive power loads of EVs, respectively.

$$P^0_{ev(n)} = \lambda_{ev} \times P^0_{L(n)} \tag{47}$$

$$Q^0_{ev(n)} = P^0_{ev(n)} \times \tan(\varphi_{n(c)}) \tag{48}$$

where $P^0_{ev(n)}$ and $Q^0_{ev(n)}$ are active and reactive powers of the additional load due to the integration of EVs at the n^{th} bus, λ_{ev} is a scale factor representing the amount of EV load compared to the actual power load at the considered placement, $P^0_{L(n)}$ is the actual nominal power of the load at the n^{th} bus, $P^0_{ev(n)}$ is the added EV load of the n^{th} bus, and $\varphi_{n(c)}$ is the AC/DC converter's power factor.

The summation of the real and reactive load powers after considering the EV penetration at different placements can be presented by the expressed equations.

$$P^t_{d(n)} = P^0_{L(n)} \times \left(\frac{V^t_{(n)}}{V^0_{(n)}}\right)^{\alpha} + \left\{P^0_{ev(n)} \times \left(\frac{V^t_{(n)}}{V^0_{(n)}}\right)^{\alpha_{ev}}\right\} \tag{49}$$

$$Q^t_{d(n)} = Q^0_{L(n)} \times \left(\frac{V^t_{(n)}}{V^0_{(n)}}\right)^{\beta} + \left\{Q^0_{ev(n)} \times \left(\frac{V^t_{(n)}}{V^0_{(n)}}\right)^{\beta_{ev}}\right\} \tag{50}$$

where $P^t_{d(n)}$ and $Q^t_{d(n)}$ are the active and reactive load powers at the nth bus after consideration in conjunction with the EV load, respectively, $Q^0_{L(n)}$ is the reactive nominal power of the load at the n^{th} bus, respectively, $V^0_{(n)}$ and $V^t_{(n)}$ are the initial and

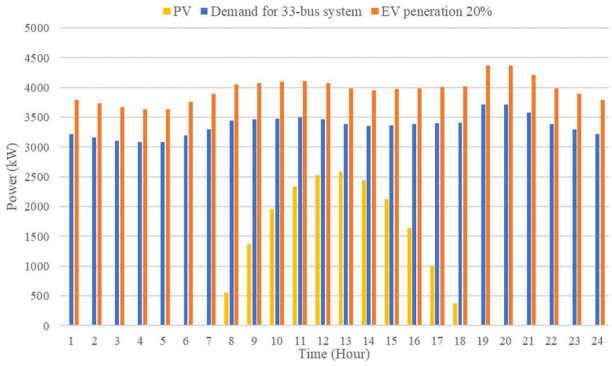

FIGURE 5. Load demand, PV profile, and EV penetration at 20% of the IEEE 33-bus distribution system [20].

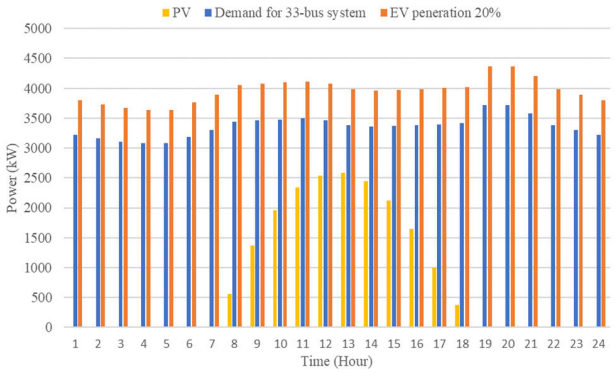

FIGURE 6. Load demand, PV profile, and EV penetration at 20% of the IEEE 69-bus distribution system [35].

time nominal voltages, respectively, $\alpha = 0$ and $\beta = 0$ are the real and reactive power exponents of the load demand, respectively, and $\alpha_{ev} = 2.59$ and $\beta_{ev} = 4.06$ are the real and reactive vehicle load exponents, respectively [36]. Fig. 5 and Fig. 6 show the load demand when the EV penetration is at 20%.

V. SIMULATION RESULTS AND DISCUSSION

The optimal placement and capacity of the BESS were simulated in the IEEE 33- and 69-bus distribution systems connected with PV and EVs in order to find the minimum costs of installation, replacement, transmission loss, voltage regulation, and peak demand. MATLAB and MATPOWER were utilized to run the simulation to simulate the power flow. The computational complexity of the proposed techniques depends on the Fourier series applied to predict the energy of the BESS in a distribution system. The Fourier series then primarily depends on the number of Fourier coefficients considered in the series. The more number of Fourier coefficients provides more accuracy of the generated solutions but also requires higher computational effort. Moreover, to compare distribution system efficiency enhancement before and after the BESS installation, three metaheuristic algorithms, including PSO, AVOA, and SSA were employed. The number of the populations and maximum iterations of algorithm operation were imposed to 60 and 250, respectively. The simulation results are presented as follows:

TABLE 2. The best fourier coefficients provided by each algorithm in the IEEE 33-bus distribution system.

Algorithms	Fourier Coefficients			
PSO	a_1	b_1	a_2	b_2
	0.10322	-1.74857	-0.70902	0.15369
	a_3	b_3	a_4	b_4
	-0.03417	0.18476	0.10263	0.03452
	a_5	b_5	a_6	b_6
	0.08428	0.02162	-0.03887	-0.04304
	a_7	b_7	a_8	b_8
	-0.00464	-0.02699	-0.01250	0.03469
AVOA	a_1	b_1	a_2	b_2
	-0.25026	-0.88360	-0.49761	0.06689
	a_3	b_3	a_4	b_4
	0.00184	0.17462	0.11483	0.01912
	a_5	b_5	a_6	b_6
	0.01037	0.01036	-0.02604	-0.01841
	a_7	b_7	a_8	b_8
	-0.00089	-0.01067	0.00674	-0.00182
SSA	a_1	b_1	a_2	b_2
	0.04825	-1069711	-0.62566	0.19301
	a_3	b_3	a_4	b_4
	-0.08193	0.07924	0.12065	0.14032
	a_5	b_5	a_6	b_6
	0.9653	-0.88260	-0.10149	0.02082
	a_7	b_7	a_8	b_8
	0.04179	-0.01961	-0.01447	0.02059

A. IEEE 33-BUS DISTRIBUTION SYSTEM

The optimal placement and capacity of the BESS were first determined to install in the IEEE 33-bus distribution system. The load data of this system was obtained from Table 1, and the loads on all buses were increased according to EV penetration by using (46)-(49). The efficiency of each algorithm is investigated after the BESS installation in terms of the minimum system costs which include the investment cost, replacement cost, and operation and maintenance costs of installing the BESS. Moreover, the efficiency enhancement of the distribution system provided by all considered algorithms was compared in terms of the VDI, transmission line loss, and maximum peak demand after the BESS installation.

1) OPTIMAL PLACEMENT AND CAPACITY OF THE BESS

The optimal placement and capacity of the BESS were evaluated in the IEEE 33-bus distribution system in order to minimize system costs which comprise investment, replacement, and operating costs by applying PSO, AVOA, and SSA. The optimized values of the decision variables, Fourier coefficients, calculated by three considered algorithms are provided in Table 2. The best Fourier coefficients obtained by each algorithm were used to determine the SOE of the BESS within 24 hours as presented in Fig. 7. The optimal

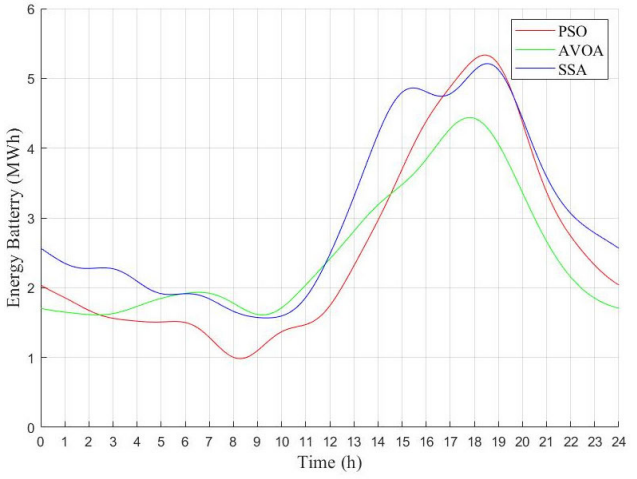

FIGURE 7. Stage of Energy (SOE) of the BESS provided by each algorithm for the IEEE 33-bus distribution system.

TABLE 3. Optimal placement and capacity of the BESS in the IEEE 33-bus distribution system.

Algorithms	Best placement	BESS size (MWh)	Power of BESS (MW)	Lifetime of BESS	System Costs ($)
PSO	6	5.3342	0.9439	8.8247	25,933,282.71
AVOA	6	4.4386	0.9426	8.7514	26,110,137.49
SSA	6	5.2113	1.0463	8.8211	25,957,185.51

placement and capacity of the BESS together with the power of the BESS, lifetime of the BESS, and system cost were then found by all considered algorithms as shown in Table 3. It was noticed that the best placements of the BESS provided by all algorithms were at bus 6 where PSO required the largest BESS size of 5.3342 MWh, followed by SSA at 5.2113 MWh, and AVOA requires the smallest size of the BESS at 4.4386 MWh, respectively. In term of the objective function, which is the system costs, PSO generated the best objective value followed by SSA and AVOA, respectively.

2) ALGORITHM EFFICIENCY COMPARISON

The efficiency enhancement of the IEEE 33-bus distribution system was evaluated by examining the VDI, transmission line loss, and maximum peak demand before and after the BESS installation by using PSO, AVOA, and SSA as presented in Table 4. It was found that after the BESS was installed in the system, all three algorithms achieved decreases in the VDI, transmission losses, and peak demand, which improved the system efficiency. PSO provided the best VDI value, followed by SSA, and AVOA, respectively. For the transmission line losses, PSO obtained the largest decrease of loss followed by AVOA and SSA, respectively. The maximum peak demands after the BESS installation were decreased with the largest reduction by PSO followed by SSA and AVOA, respectively.

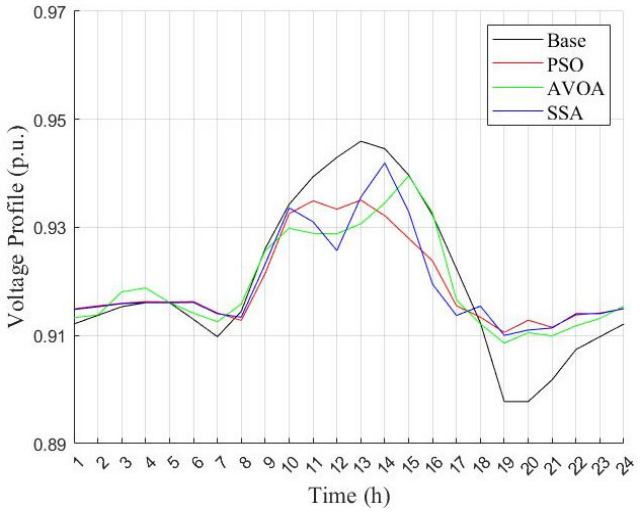

FIGURE 8. Voltage profile comparison of the 18th bus for the IEEE 33-bus system.

TABLE 4. Efficiency comparison of the BESS installation in the IEEE 33-bus distribution system.

Algorithms	VDI (%)	Real power loss (MW)	Reactive power loss (MVAr)	Apparent power loss (MVA)	Maximum peak Demand (MW)
Base	200.2029	4.4743	3.0297	5.4036	4.6484
PSO	172.1783	4.2803	2.9046	5.1728	3.8197
AVOA	176.5046	4.2925	2.9125	5.1873	3.9286
SSA	173.2407	4.2934	2.9130	5.1883	3.8288

The enhancement of the 24-hour voltage profile at the 18th bus, which is the weakest bus before and after the BESS installation by each algorithm is shown in Fig. 8. It is observed that the voltage was lower than the lower voltage constraint from 7:00 p.m. to 8:00 p.m. in the base case and could be increased to be within the constraints after installing the BESS by all considered algorithms. Fig. 9 presents the voltage profile of all buses in the system at 8:00 p.m., which was the time when the peak demand was required in a day. It can be seen that the voltage was the lowest in the 18th bus because it was the farthest bus from the reference bus, and after installing the BESS, it can be seen that the voltage in the 18th bus was improved to be within the constraints.

To investigate the transmission loss at each hour after installing the BESS by all algorithms, real power loss with a day in this system is plotted in Fig. 10. The loss slightly decreased when compared to the base case from 1:00 a.m. to 8:00 a.m. and increased more than the base case from 8:00 a.m. to 6:00 p.m. because the BESS was in the charging state to reserve power for peak times. The loss was significantly reduced from 6:00 p.m. to 0:00 a.m. because the BESS discharged power to supply the load demand together with the grid. So, the overall 24-hour transmission line loss of the distribution system was decreased after the BESS installation compared to the base case.

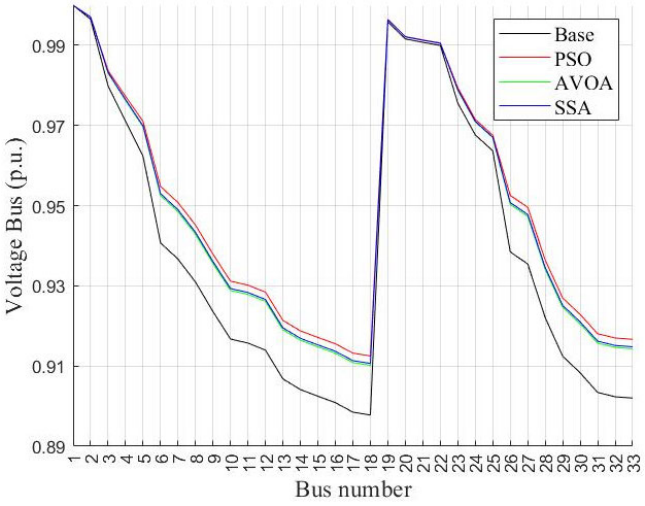

FIGURE 9. Voltage profile comparison of all buses at 8.00 p.m. for the IEEE 33-bus.

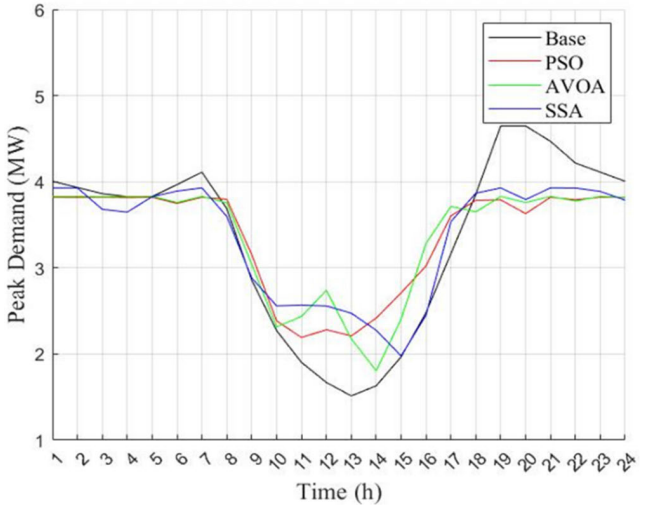

FIGURE 11. Peak demand comparison for the IEEE 33-bus system.

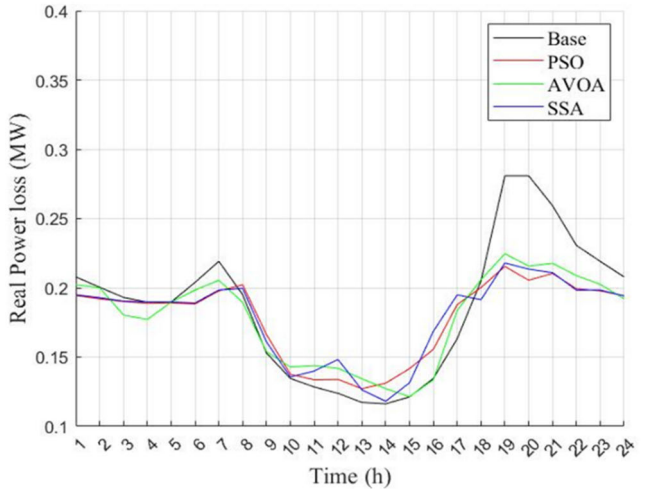

FIGURE 10. Real power loss comparison for the IEEE 33-bus system.

Fig. 11 expresses the comparison of peak demand for the IEEE 33-bus distribution system to evaluate the peak demand enhancement after the BESS installation. Peak demand for the base case was at its highest at 8:00 p.m., as well as from 1 a.m. to 8:00 a.m. and from 6:00 p.m. to 0:00 a.m. It can be seen that the peak demand after installing the BESS by all considered algorithms was improved to be less than the base case because the BESS was supplied together with the power from the grid. From 8:00 a.m. to 6:00 p.m., the peak demand was higher than the base case because BESS was in the charging state to store power for supply during the peak time.

3) COMPARISONS OF ALGORITHM PERFORMANCE

To further investigate and validate the efficiency after the optimal placement and capacity of the BESS installation obtained from the algorithms, the statistical analysis, operation times convergence curves of the minimum costs and payback period are presented. The statistical results including best value, worst value, mean, median and standard deviation of the objective values generated by each algorithm together with operation times are expressed in Table 5. It is noticed that PSO gave the best values in all aspects except for standard deviation while AVOA generated the best standard deviation. However, SSA consumed the shortest operation time followed by PSO and AVOA. The comparison results of system costs converging for 250 iterations of the considered algorithms are shown in Fig. 12. When the BESS was installed on the 6th bus, PSO generated the most effective system costs, followed by SSA and AVOA, respectively, and PSO was also the fastest one to converge to the minimum objective value. After that, the obtained information was used to calculate the break-even point for investment consideration. The break-even point was calculated by the installation costs of the BESS divided by the difference between the O&M costs of the system before and after the BESS installation. The results are presented in Table 6, where BESS installed by using AVOA showed the fastest payback period, followed by SSA and PSO, respectively, because AVOA has the smallest size of the BESS compared to the other algorithms according to Table 3, resulting in BESS installation using a lower budget.

B. IEEE 69-BUS DISTRIBUTION SYSTEM

To confirm the efficiency of the proposed method in a larger system, the IEEE-69 bus distribution system was tested to determine the optimal placement and capacity of the BESS in the distribution system. The load data of this system is provided in Table 1. The simulation results of this system are presented in the subsequent sections.

1) OPTIMAL PLACEMENT AND CAPACITY OF THE BESS

To determine the optimal capacity and placement of the BESS with minimum system costs in the IEEE 69-bus system, the optimized values of the decision variables, which are

TABLE 5. Statistical results of each algorithm in the IEEE 33-bus distribution system.

Algorithms	PSO	AVOA	SSA
Best	25,933,282.71	26,110,137.49	25,957,185.51
Worst	26,200,842.01	26,393,674.66	26,633,224.01
Mean	26,040,010.76	26,209,077.01	26,236,034.25
Median	26,014,139.99	26,186,509.77	26,157,091.50
Std.	87,562.67	79,907.06	203,617.23
Time (s)	23,242.32	23,392.12	23,227.05

TABLE 6. System cost and payback period comparison of the IEEE 33-bus distribution system.

Algorithms	System costs ($)	Operation and maintenance costs for 1 day ($)	Payback (year)
Base	-	3,823.00	-
PSO	25,933,282.71	3,313.82	2.8702
AVOA	26,110,137.49	3,376.97	2.7264
SSA	25,957,185.51	3,322.53	2.8529

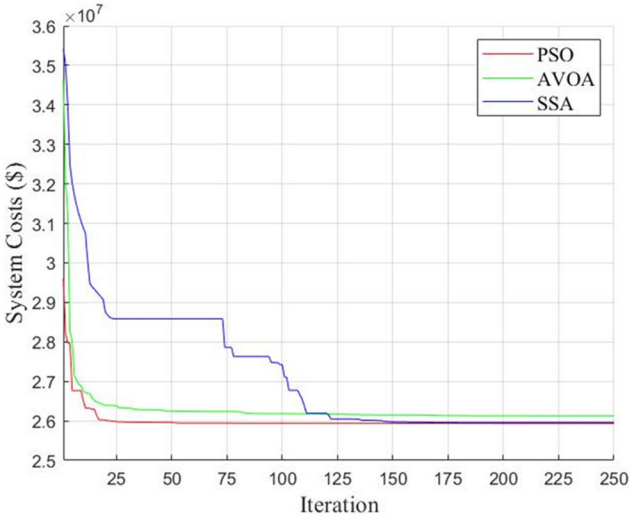

FIGURE 12. Convergence curves of the system costs of each algorithm for the IEEE 33-bus system.

TABLE 7. The best Fourier coefficients provided by each algorithm in the IEEE 69-bus distribution system.

Algorithms	Fourier Coefficients			
PSO	a_1	b_1	a_2	b_2
	-0.09183	-1.25233	-0.69867	0.07528
	a_3	b_3	a_4	b_4
	-0.00346	0.21159	0.10899	0.00227
	a_5	b_5	a_6	b_6
	0.00572	0.06526	0.06811	-0.05842
	a_7	b_7	a_8	b_8
	-0.05844	-0.04646	-0.00705	0.05010
AVOA	a_1	b_1	a_2	b_2
	-0.04958	-0.97433	-0.60675	0.00536
	a_3	b_3	a_4	b_4
	-0.03994	0.23192	0.13353	0.04209
	a_5	b_5	a_6	b_6
	-0.00052	-0.00928	0.02007	-0.03136
	a_7	b_7	a_8	b_8
	-0.01360	-0.02457	-0.00842	0.02156
SSA	a_1	b_1	a_2	b_2
	-0.32422	-1.11871	-0.54196	0.19744
	a_3	b_3	a_4	b_4
	-0.03062	0.08279	0.13438	0.06685
	a_5	b_5	a_6	b_6
	-0.00445	-0.03240	-0.01543	-0.00902
	a_7	b_7	a_8	b_8
	0.00661	0.02062	-0.00521	-0.00550

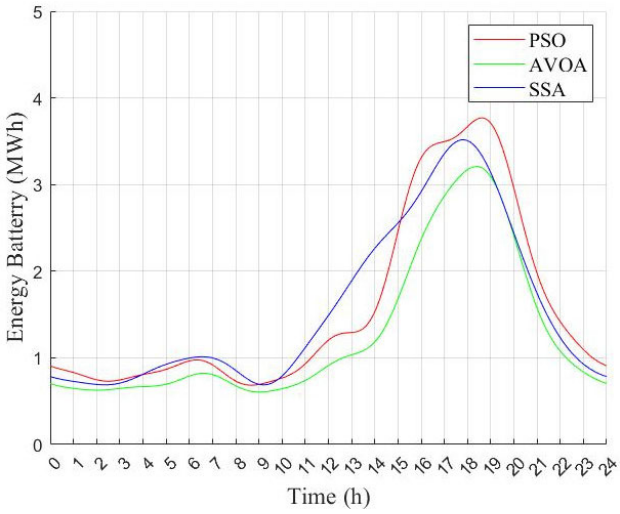

FIGURE 13. SOE of the BESS provided by each algorithm for the IEEE 69-bus distribution system.

the Fourier coefficients, generated by three considered algorithms are found as shown in Table 7. The battery energy in the 24-hour period was then calculated by using the Fourier coefficients, and the states of energy provided by each considered algorithm were plotted as in Fig. 13. The placement of the BESS installation provided by PSO was at the 54th bus and at the 55th bus for both AVOA and SSA. The placement, capacity, power, lifetime, and system costs of the BESS provided by each algorithm are presented in Table 8. It was found that PSO required the largest BESS size of 3.7692 MWh, followed by SSA at 3.5166 MWh and AVOA at 3.2089 MWh, respectively. For the system costs, PSO obtained the best costs followed by AVOA and SSA, respectively.

C. ALGORITHM EFFICIENCY COMPARISON

The efficiency of all algorithms in the ieee 69-bus distribution system is evaluated by examining the vdi, transmission losses, and maximum peak demand before and after the

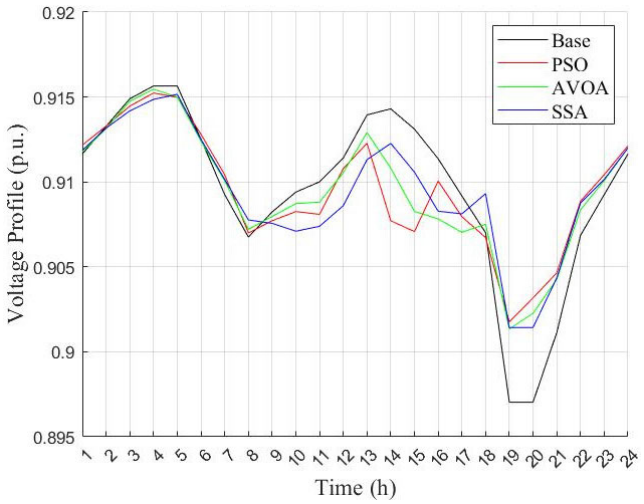

FIGURE 14. Voltage profile comparison of the 65th bus for the IEEE 69-bus system.

TABLE 8. Optimal placement and capacity of the BESS in the IEEE 69-bus distribution system.

Algorithms	Best placement	BESS size (MWh)	Power of BESS (MW)	Lifetime of BESS	System Costs ($)
PSO	54	3.7692	0.9769	8.2254	29,572,175.59
AVOA	55	3.2089	0.7901	8.2456	29,603,862.21
SSA	55	3.5166	0.6611	7.9646	29,680,415.60

TABLE 9. Efficiency comparison of the bess installation in the IEEE 69-bus distribution system.

Algorithms	VDI (%)	Real power loss (MW)	Reactive power loss (MVAr)	Apparent power loss (MVA)	Maximum peak Demand (MW)
Base	216.4787	5.8152	2.6273	6.3812	4.7834
PSO	199.6260	5.8202	2.6286	6.3863	4.0415
AVOA	199.0248	5.8213	2.6294	6.3875	4.0974
SSA	197.4168	5.8195	2.6283	6.3855	4.0836

installation of the bess as presented in Table 9. By evaluating the comparison of the vdi, it was observed that when bess was installed in the distribution system, all three algorithms resulted in a vdi reduction, which was advantageous to the distribution system. The best vdi was obtained by ssa followed by avoa, and pso, respectively. It was observed that the bess installation cannot decrease transmission losses in the ieee 69-bus distribution systems. This is because, during the period between 1:00 A.M. to 6:00 A.M. and 8:00 A.M. to 6:00 P.M., The bess was charging to reserve power to decrease peak demand during the peak demand period from 6:00 P.M. to 0:00 A.M. In term of peak demand reduction comparison, the highest reduction of peak demand was provided by pso, followed by ssa and avoa, respectively.

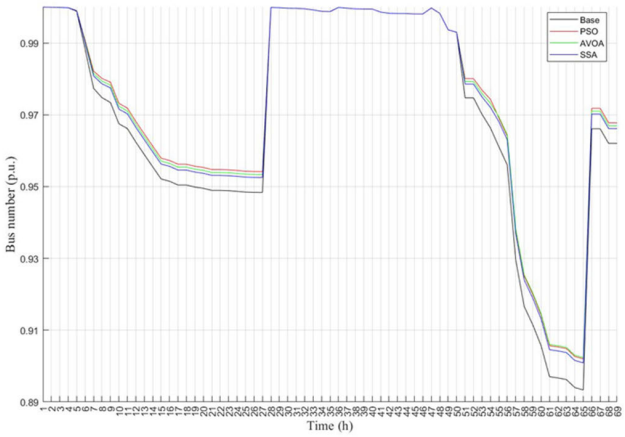

FIGURE 15. Voltage profile comparison of all buses at 8.00 p.m. for the IEEE 69-bus system.

TABLE 10. Statistical results of each algorithm in the IEEE 69-bus distribution system.

Algorithms	PSO	AVOA	SSA
Best	29,572,175.60	29,603,862.21	29,680,415.59
Worst	29,957,728.13	30,046,106.10	32,959,028.38
Mean	29,721,951.40	29,780,709.30	30,592,240.12
Median	29,671,100.87	29,756,369.56	30,348,051.77
Std.	130,722.10	111,396.71	992,083.15
Time (s)	59,299.55	60,141.59	56,469.76

The voltage profile of the weakest bus, which is the 65th bus over 24 hours, is displayed in Fig. 14 to illustrate the enhancement in the voltage profile after the bess installation by all considered algorithms. It is noticeable that between 7:00 P.M. and 8:00 P.M., The voltage for a base case was lower than the lower voltage constraint; however, it can be improved within the constraints once bess was installed. Fig. 15 presents the voltage profile of all buses to observe the overall voltage enhancement of the system when the majority of a load demand was required at 8:00 P.M. it is noticed that the 65th bus had the lowest voltage which was below the voltage constraint because it was the farthest bus from the reference bus. However, after installing the bess in the optimal placement, the voltage profile at the 65th bus increased more than the base case and within the constraints.

The transmission real power loss in the IEEE 69-bus distribution system is shown in Fig. 16 to notice the line loss at each hour. It is noticed that from 1:00 a.m. to 6:00 a.m. and 8:00 a.m. to 6:00 p.m., the transmission line loss increased more than the base case since the BESS was in the charging state to reserve power for the peak demand period. However, the loss was significantly reduced from 6:00 p.m. to 0:00 a.m. because the BESS discharged power to help supply the system together with the grid. As a result, the overall 24-hour

TABLE 11. System cost and payback period comparison of the IEEE 69-bus distribution system.

Algorithms	System costs ($)	Operation and maintenance costs for 1 day ($)	Payback (year)
Base	-	4,278.9010	-
PSO	29,572,175.59	3,872.9910	2.5440
AVOA	29,603,862.21	3,904.7884	2.3493
SSA	29,680,415.60	3,896.6692	2.5206

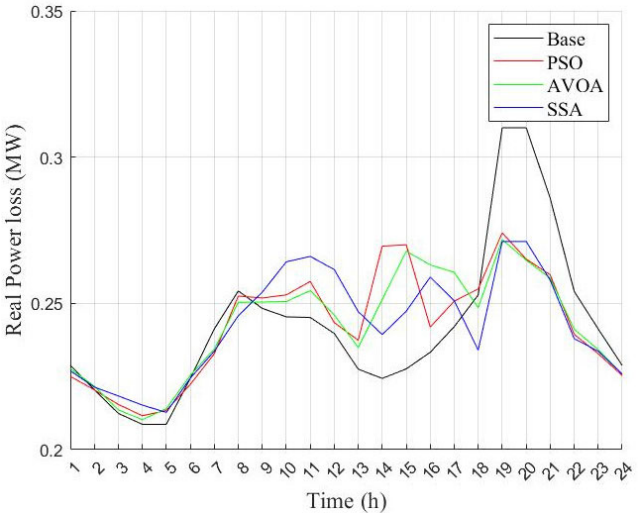

FIGURE 16. Real power loss comparison for the IEEE 69-bus system.

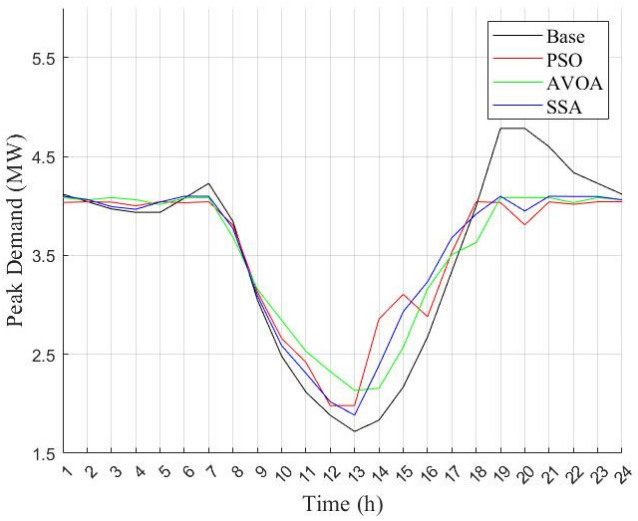

FIGURE 17. Peak demand comparison for the IEEE 69-bus system.

transmission line loss of the distribution system was not decreased compared with that of the base case.

Peak demands for the IEEE 69-bus distribution system before and after the BESS installation by the considered algorithms are compared in Fig. 17. It is seen that the base case had the highest peak demand at 8:00 p.m. It can be observed that from 1:00 a.m. to 6:00 a.m. and 8:00 a.m. to 6:00 p.m., peak demand after the BESS installation was higher than that of the base case because BESS charged backup power to decrease peak demand during the peak load. So, peak demand when installing the BESS was significantly improved from that of the base case between 6:00 p.m. to 0:00 a.m. and slightly enhanced from the base case between 6:00 to 8:00 a.m. Consequently, the overall 24-hour peak demand after installing the BESS by all algorithms could be decreased.

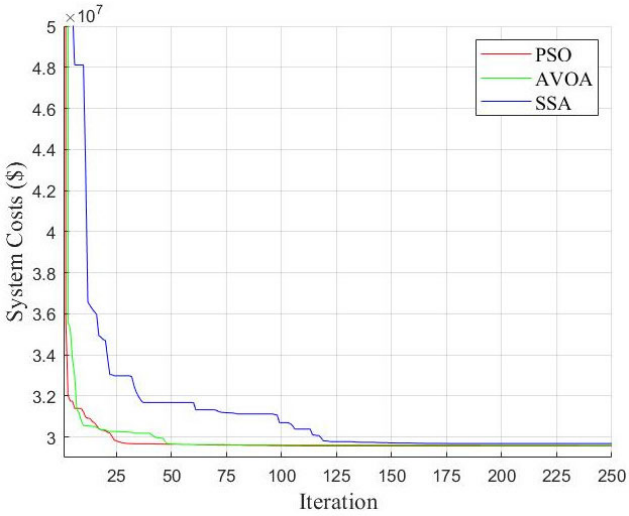

FIGURE 18. Convergence curves of the system costs of each algorithm for the IEEE 69-bus system.

1) COMPARISONS OF ALGORITHM PERFORMANCE

To compare the efficiency of the considered algorithms to determine the optimal placement and capacity of the BESS in the IEEE 69-bus system, the statistical results and operation times of all algorithms are presented in Table 10, the convergence curves presenting the minimum system costs over 20 years of each algorithm are shown in Fig. 18, and the payback period is also compared. From the statistical results in Table 10, PSO generated the best values in best, worst, mean, and median values followed by AVOA and SSA while AVOA obtained the best standard deviation value followed by PSO and SSA. SSA used the fastest operation time followed by PSO while AVOA consumed the longest time. For the convergence curves in Fig. 18, it is seen that PSO was the first algorithm to converge to the optimal solution followed by AVOA and SSA, respectively. The break-even point for investment consideration was investigated as presented in Table 11, where BESS installed using AVOA showed the fastest payback period, followed by SSA and PSO, respectively, because AVOA has the smallest size of the BESS compared to the other algorithms according to Table 8. As a result, PSO provided the best costs in terms of technical price and AVOA gave the best cost in terms of economic price.

VI. CONCLUSION

This study presents an approach for determining the optimal placement and capacity of the BESS to minimize the

system costs and improve the efficiency of the distribution systems integrated with PV and EVs. The main objective function is to minimize system costs, including installation, replacement, transmission loss, voltage regulation, and peak demand costs while ensuring optimal control by considering the voltage of all buses, battery power, and energy battery as constraints. Three metaheuristic algorithms comprising PSO, AVOA, and SSA are used to solve the optimization problem, and the IEEE 33- and 69-bus distribution systems are tested. In the IEEE 33-bus system, the results show that PSO could obtain the optimal placement and capacity of the BESS with the best system costs followed by AVOA and SSA, respectively. PSO also provided the best VDI, decreasing of transmission loss, and decreasing of peak demand after the BESS installation followed by AVOA and SSA in term of loss reduction and SSA and AVOA in term of peak demand reduction while AVOA achieved the fastest payback period followed by SSA and PSO. The statistical results of PSO are the best compared to the other algorithms except for standard deviation which AVOA provided the best while SSA used the fastest operation time. It is also found that installing the BESS by all considered algorithms could move the voltage of all buses from the base case to be within the constraints. The simulation results of the IEEE 69-bus system express that PSO provided the best system costs for giving the optimal placement and capacity of the BESS followed by AVOA and SSA, respectively. The efficiency comparison in this system found that SSA obtained the least VDI followed by AVOA and PSO while PSO achieved the best maximum peak demand reduction followed by SSA and AVOA, and AVOA provided the fastest payback period followed by SSA and PSO. PSO also generated the best values in all aspects of the statistical results except for standard deviation while AVOA generated the best standard deviation and SSA consumed the shortest operation time. The out-of-range bus voltages of the base case could also move to be within the constraints after the BESS installation by each algorithm. However, the overall transmission line losses after the BESS installation provided by all considered algorithms were close to those of the base because the IEEE 69-bus system is too large for only one installation BESS. The results show that it is not always necessary to install BESS on the same bus as the PV when the distribution system is larger. In future work, the optimal placement and capacity of more than one BESSs will be considered for installation in distribution systems to evaluate system efficiency enhancement and system costs.

REFERENCES

[1] A. Raihan and A. Tuspekova, "Dynamic impacts of economic growth, energy use, urbanization, tourism, agricultural value-added, and forested area on carbon dioxide emissions in Brazil," *J. Environ. Stud. Sci.*, vol. 12, no. 4, pp. 794–814, Dec. 2022, doi: 10.1007/s13412-022-00782-w.

[2] M. S. Hassan, H. Mahmood, and A. Javaid, "The impact of electric power consumption on economic growth: A case study of Portugal, France, and Finland," *Environ. Sci. Pollut. Res.*, vol. 29, no. 30, pp. 45204–45220, Jun. 2022, doi: 10.1007/s11356-022-19097-y.

[3] M. Kongkuah, H. Yao, and V. Yilanci, "The relationship between energy consumption, economic growth, and CO_2 emissions in China: The role of urbanisation and international trade," *Environ., Develop. Sustainability*, vol. 24, no. 4, pp. 4684–4708, Apr. 2022, doi: 10.1007/s10668-021-01628-1.

[4] Q. Dai, J. Liu, and Q. Wei, "Optimal photovoltaic/battery energy storage/electric vehicle charging station design based on multi-agent particle swarm optimization algorithm," *Sustainability*, vol. 11, no. 7, p. 1973, Apr. 2019, doi: 10.3390/su11071973.

[5] M. Motalleb, E. Reihani, and R. Ghorbani, "Optimal placement and sizing of the storage supporting transmission and distribution networks," *Renew. Energy*, vol. 94, pp. 651–659, Aug. 2016, doi: 10.1016/j.renene.2016.03.101.

[6] S. A. El-Batawy and W. G. Morsi, "Optimal design of community battery energy storage systems with prosumers owning electric vehicles," *IEEE Trans. Ind. Informat.*, vol. 14, no. 5, pp. 1920–1931, May 2018, doi: 10.1109/TII.2017.2752464.

[7] D. M. Tovilovic and N. L. Rajakovic, "The simultaneous impact of photovoltaic systems and plug-in electric vehicles on the daily load and voltage profiles and the harmonic voltage distortions in urban distribution systems," *Renew. Energy*, vol. 76, pp. 454–464, Apr. 2015, doi: 10.1016/j.renene.2014.11.065.

[8] O. Babacan, W. Torre, and J. Kleissl, "Siting and sizing of distributed energy storage to mitigate voltage impact by solar PV in distribution systems," *Sol. Energy*, vol. 146, pp. 199–208, Apr. 2017, doi: 10.1016/j.solener.2017.02.047.

[9] C. K. Das, O. Bass, G. Kothapalli, T. S. Mahmoud, and D. Habibi, "Overview of energy storage systems in distribution networks: Placement, sizing, operation, and power quality," *Renew. Sustain. Energy Rev.*, vol. 91, pp. 1205–1230, Aug. 2018, doi: 10.1016/j.rser.2018.03.068.

[10] B. G. Desai, "Electrical energy storage," IEC, Geneva, Switzerland, White Paper, 1981, vol. 1, no. 3, doi: 10.1049/pbpo167e_ch7.

[11] P. Boonluk, A. Siritaratiwat, P. Fuangfoo, and S. Khunkitti, "Optimal siting and sizing of battery energy storage systems for distribution network of distribution system operators," *Batteries*, vol. 6, no. 4, p. 56, 2020, doi: 10.3390/batteries6040056.

[12] A. Fathy, "A novel artificial hummingbird algorithm for integrating renewable based biomass distributed generators in radial distribution systems," *Appl. Energy*, vol. 323, Oct. 2022, Art. no. 119605, doi: 10.1016/j.apenergy.2022.119605.

[13] M. A. Tolba, E. H. Houssein, A. A. Eisa, and F. A. Hashim, "Optimizing the distributed generators integration in electrical distribution networks: Efficient modified forensic-based investigation," *Neural Comput. Appl.*, vol. 35, no. 11, pp. 8307–8342, Apr. 2023, doi: 10.1007/s00521-022-08103-6.

[14] N. Jayasekara, M. A. S. Masoum, and P. J. Wolfs, "Optimal operation of distributed energy storage systems to improve distribution network load and generation hosting capability," *IEEE Trans. Sustain. Energy*, vol. 7, no. 1, pp. 250–261, Jan. 2016, doi: 10.1109/TSTE.2015.2487360.

[15] A. Mazza, H. Mirtaheri, G. Chicco, A. Russo, and M. Fantino, "Location and sizing of battery energy storage units in low voltage distribution networks," *Energies*, vol. 13, no. 1, p. 52, 2019, doi: 10.3390/en13010052.

[16] A. Ahmadian, M. Sedghi, and M. Aliakbar-Golkar, "Fuzzy load modeling of plug-in electric vehicles for optimal storage and DG planning in active distribution network," *IEEE Trans. Veh. Technol.*, vol. 66, no. 5, pp. 3622–3631, May 2017, doi: 10.1109/TVT.2016.2609038.

[17] M. Khalid, U. Akram, and S. Shafiq, "Optimal planning of multiple distributed generating units and storage in active distribution networks," *IEEE Access*, vol. 6, pp. 55234–55244, 2018, doi: 10.1109/ACCESS.2018.2872788.

[18] Y. Zheng, Y. Song, A. Huang, and D. J. Hill, "Hierarchical optimal allocation of battery energy storage systems for multiple services in distribution systems," *IEEE Trans. Sustain. Energy*, vol. 11, no. 3, pp. 1911–1921, Jul. 2020, doi: 10.1109/TSTE.2019.2946371.

[19] S. Khunkitti, P. Boonluk, and A. Siritaratiwat, "Optimal location and sizing of BESS for performance improvement of distribution systems with high DG penetration," *Int. Trans. Electr. Energy Syst.*, vol. 2022, pp. 1–16, Jun. 2022, doi: 10.1155/2022/6361243.

[20] V. Janamala and D. S. Reddy, "Coyote optimization algorithm for optimal allocation of interline—Photovoltaic battery storage system in islanded electrical distribution network considering EV load penetration," *J. Energy Storage*, vol. 41, Sep. 2021, Art. no. 102981, doi: 10.1016/j.est.2021.102981.

[21] D. Sadeghi, A. H. Naghshbandy, and S. Bahramara, "Optimal sizing of hybrid renewable energy systems in presence of electric vehicles using multi-objective particle swarm optimization," *Energy*, vol. 209, Oct. 2020, Art. no. 118471, doi: 10.1016/j.energy.2020.118471.
[22] R. Eberhart and J. Kennedy, "A new optimizer using particle swarm theory," in *Proc. 6th Int. Symp. Micro Mach. Human Sci.*, 1995, pp. 39–43, doi: 10.1109/MHS.1995.494215.
[23] B. Abdollahzadeh, F. S. Gharehchopogh, and S. Mirjalili, "African vultures optimization algorithm: A new nature-inspired metaheuristic algorithm for global optimization problems," *Comput. Ind. Eng.*, vol. 158, Aug. 2021, Art. no. 107408, doi: 10.1016/j.cie.2021.107408.
[24] S. Mirjalili, A. H. Gandomi, S. Z. Mirjalili, S. Saremi, H. Faris, and S. M. Mirjalili, "Salp swarm algorithm: A bio-inspired optimizer for engineering design problems," *Adv. Eng. Softw.*, vol. 114, pp. 163–191, Dec. 2017, doi: 10.1016/j.advengsoft.2017.07.002.
[25] F. R. McLarnon and E. J. Cairns, "Energy storage | energy storage," *Annu. Rev. Energy*, vol. 14, pp. 241–271, Nov. 1989.
[26] T. Kousksou, P. Bruel, A. Jamil, T. El Rhafiki, and Y. Zeraouli, "Energy storage: Applications and challenges," *Sol. Energy Mater. Sol. Cells*, vol. 120, pp. 59–80, Jan. 2014, doi: 10.1016/j.solmat.2013.08.015.
[27] M. Y. Suberu, M. W. Mustafa, and N. Bashir, "Energy storage systems for renewable energy power sector integration and mitigation of intermittency," *Renew. Sustain. Energy Rev.*, vol. 35, pp. 499–514, Jul. 2014, doi: 10.1016/j.rser.2014.04.009.
[28] M. Stecca, L. R. Elizondo, T. B. Soeiro, P. Bauer, and P. Palensky, "A comprehensive review of the integration of battery energy storage systems into distribution networks," *IEEE Open J. Ind. Electron. Soc.*, vol. 1, pp. 46–65, 2020, doi: 10.1109/OJIES.2020.2981832.
[29] P. Boonluk, S. Khunkitti, P. Fuangfoo, and A. Siritaratiwat, "Optimal siting and sizing of battery energy storage: Case study seventh feeder at Nakhon Phanom substation in Thailand," *Energies*, vol. 14, no. 5, p. 1458, Mar. 2021, doi: 10.3390/en14051458.
[30] P. Wolfs, N. Jayasekera, and S. Subawickrama, "A Fourier series based approach to the periodic optimisation of finely dispersed battery storage," in *Proc. AUPEC*, Sep. 2011, pp. 1–6.
[31] N. Ghorbani, A. Kasaeian, A. Toopshekan, L. Bahrami, and A. Maghami, "Optimizing a hybrid wind-PV-battery system using GA-PSO and MOPSO for reducing cost and increasing reliability," *Energy*, vol. 154, pp. 581–591, Jul. 2018, doi: 10.1016/j.energy.2017.12.057.
[32] L. Abualigah and M. Altalhi, "A novel generalized normal distribution arithmetic optimization algorithm for global optimization and data clustering problems," *J. Ambient Intell. Humanized Comput.*, vol. 14, pp. 1–29, May 2022. [Online]. Available: https://link.springer.com/journal/12652/volumes-and-issues, doi: 10.1007/s12652-022-03898-7.
[33] X. Chen, K. Ding, J. Zhang, Z. Yang, Y. Liu, and H. Yang, "A two-stage method for model parameter identification based on the maximum power matching and improved flow direction algorithm," *Energy Convers. Manag.*, vol. 278, Feb. 2023, Art. no. 116712, doi: 10.1016/j.enconman.2023.116712.
[34] M. E. Baran and F. F. Wu, "Network reconfiguration in distribution systems for loss reduction and load balancing," *IEEE Power Eng. Rev.*, vol. 9, no. 4, pp. 101–102, Apr. 1989, doi: 10.1109/MPER.1989.4310642.
[35] M. E. Baran and F. F. Wu, "Optimal capacitor placement on radial distribution systems," *IEEE Trans. Power Del.*, vol. 4, no. 1, pp. 725–734, Jan. 1989, doi: 10.1109/61.19265.
[36] S. Satyanarayana, T. Ramana, S. Sivanagaraju, and G. K. Rao, "An efficient load flow solution for radial distribution network including voltage dependent load models," *Electric Power Compon. Syst.*, vol. 35, no. 5, pp. 539–551, May 2007, doi: 10.1080/15325000601078179.

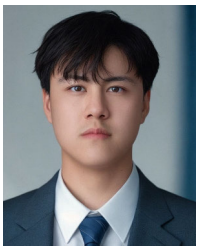

NATSAWAT POMPERN (Member, IEEE) was born in Phitsanulok, Thailand, in 1993. He received the B.Eng. degree in electrical engineering from the King Mongkut's Institute of Technology Ladkrabang (KMITL), in 2015. He is currently pursuing the master's degree with the Department of Electrical Engineering, Chiang Mai University. Since 2018, he has been an Electrical Engineer with the Provincial Electricity Authority (PEA), Thailand. His research interests include battery energy storage systems, electric vehicles, optimization, metaheuristic algorithms, temperature control, ventilation systems, and programmable logic controller.

SUTTICHAI PREMRUDEEPREECHACHARN received the B.Eng. degree in electrical engineering from Chiang Mai University, Thailand, in 1988, and the M.S. and Ph.D. degrees in electric power engineering from the Rensselaer Polytechnic Institute, Troy, NY, USA, in 1992 and 1997, respectively. He is currently an Associate Professor with the Department of Electrical Engineering, Chiang Mai University. His research interests include renewable energy, power quality, high-quality utility interface, power electronics, and artificial intelligence applied to power systems.

APIRAT SIRITARATIWAT was born in Maha Sarakham, Thailand, in 1970. He received the B.Eng. degree in electrical engineering from Khon Kaen University, Thailand, in 1992, and the Ph.D. degree in electrical engineering from The University of Manchester, U.K., in 1998. Since then, he has carried with his researches on GMR films and magnetic recording heads at HDD, Thailand. He is currently a Professor with the Department of Electrical Engineering, Khon Kaen University. His current research interests include electromagnetics, electric machine design, smart grid, and power system optimization.

SIROTE KHUNKITTI was born in Khon Kaen, Thailand, in 1993. He received B.Eng. and Ph.D. degrees in electrical engineering from Khon Kaen University (KKU), in 2014 and 2018, respectively. He is currently an Assistant Professor with the Department of Electrical Engineering, Chiang Mai University. His research interests include battery energy storage systems, electric vehicles, power system planning and optimization, and metaheuristic algorithms.